

Charmonium dissociation and recombination at RHIC and LHC

A. Capella¹, L. Bravina^{2,3}, E.G. Ferreira⁴,
A.B. Kaidalov⁵, K. Tywoniuk^{*2}, E. Zabrodin^{2,3}

¹ Laboratoire de Physique Théorique[†], Université de Paris XI, Bâtiment 210,
91405 Orsay Cedex, France

² Department of Physics, University of Oslo
0316 Oslo, Norway

³ Institute of Nuclear Physics, Moscow State University
RU-119899 Moscow, Russia

⁴ Departamento de Física de Partículas, Universidad de Santiago de Compostela,
15782 Santiago de Compostela, Spain

⁵ Institute of Theoretical and Experimental Physics
RU-117259 Moscow, Russia

Abstract

Charmonium production at heavy-ion colliders is considered within the comovers interaction model. The formalism is extended by including possible secondary J/ψ production through recombination and an estimate of recombination effects is made with no free parameters involved. The comovers interaction model also includes a comprehensive treatment of initial-state nuclear effects, which are discussed in the context of such high energies. With these tools, the model properly describes the centrality and the rapidity dependence of experimental data at RHIC energy, $\sqrt{s} = 200$ GeV, for both $Au+Au$ and $Cu+Cu$ collisions. Predictions for LHC, $\sqrt{s} = 5.5$ TeV, are presented and the assumptions and extrapolations involved are discussed.

LPT Orsay 07-125
December 2007

^{*}*E-mail address:* konrad@fys.uio.no (K. Tywoniuk).

[†]Unité Mixte de Recherche UMR n° 8627 - CNRS

1 Introduction

Disentangling effects related to the production of charmonium in hadronic collisions has been a major task for both experimentalists and theoreticians for the last two decades. The discovery of J/ψ suppression, with respect to heavy lepton pair production, in proton-nucleus (pA) collisions has been interpreted as a result of the multiple scattering of a $c\bar{c}$ pair escaping the nuclear environment – the so-called nuclear absorption. Moreover, in high energy nucleus-nucleus ($A+A$) collisions one hopes to achieve such large temperatures and densities that a new state of deconfined QCD matter, the quark-gluon plasma (QGP), is produced. It was suggested that, in the presence of a QGP, the charmonium yield would be further suppressed due to color Debye screening [1]. Indeed, such an anomalous, compared to absorption, suppression was observed in $Pb+Pb$ collisions at top SPS energy [2]. Alternatively, the SPS experimental results can also be described in terms of final state interactions of the $c\bar{c}$ pairs with the dense medium created in the collision, the so-called comovers interaction model (CIM). This model does not assume thermal equilibrium and, thus, does not use thermodynamical concepts. Within this model the SPS experimental data can be reproduced with an effective dissociation cross section $\sigma_{co} = 0.65$ mb [3].

The theoretical extrapolations to collider energies are guided mainly by two trends. On the one hand, models assuming a deconfined phase during the collision pointed to the growing importance of secondary J/ψ production due to recombination of $c\bar{c}$ pairs in the plasma. The total amount of $c\bar{c}$ pairs is assumed to be created in hard interactions during the early stages of the collision. Then, either using kinetic theory and solving rate equations for the subsequent dissociation and recombination of charmonium [4, 5], or assuming statistical coalescence at freeze-out [6, 7, 8], one obtains the final J/ψ yield. These models predict a disappearance of the charmonium suppression with rising collision energy as the lifetime of the plasma phase is expected to grow accordingly. See, however, [9] where thermal equilibrium is not assumed and charmonium dissociation is quite large at RHIC. On the other hand, the CIM with only dissociation of J/ψ 's predicts [10] a stronger suppression at RHIC than at SPS due to a larger density of produced soft particles in the collision. It also predicts a stronger suppression at $y = 0$ (where the comovers density is maximal) than at forward rapidities.

In this context, measurements of J/ψ production in $Au+Au$ collisions at RHIC, $\sqrt{s} = 200$ GeV, gave interesting although surprising results - the suppression at mid-rapidity was on the same level as at SPS [11, 12]. This was also the case for $Cu+Cu$ collisions at the same energy [13]. Furthermore, the suppression at forward rapidity in $Au+Au$ collisions was stronger than at mid-rapidity. The latter feature was not seen for the much smaller collision system created in $Cu+Cu$ collisions.

The CIM is based on the well known gain and loss differential equations in transport theory. The introduction of a recombination term is actually required for detailed balance. So far it had not been introduced in the model just because its effect was assumed to be small. The aforementioned RHIC results prompt us to a careful evaluation of the effect of the recombination (gain) term. If its effect is not negligible it will increase the final J/ψ yield. Moreover, this increase will be larger at $y = 0$ than at forward rapidities due to the narrow rapidity distribution of charm, and thus complies with RHIC data.

In the present work we will extend the CIM by allowing recombination of $c\bar{c}$ pairs into secondary J/ψ 's. We will estimate this effect using the density of charm in proton-proton (pp) collisions at the same energy and at various rapidities. Therefore, the model does not involve any additional parameters. In Section 2 we present the details of the model; both nuclear effects related to the initial state at high energy and final state interactions are described. We calculate recombination effects at mid- and forward rapidities in $Au+Au$ and $Cu+Cu$ collisions at RHIC energy $\sqrt{s} = 200$ GeV in Section 3. The suppression, found without any tuning of the parameters in the model, is in good agreement with the data. In Section 4 we make predictions for $Pb+Pb$ collisions at LHC, $\sqrt{s} = 5.5$

TeV, and discuss uncertainties related to this extrapolation. Finally, conclusions and final remarks are given in Section 5.

2 Description of the model

In this section, we give a short and updated description of the CIM which has been used to make predictions for J/ψ production in $A+A$ collisions at RHIC [10]. This model contains a comprehensive treatment of initial-state nuclear effects, such as nuclear shadowing and nuclear absorption, and final state interactions with the co-moving matter. Here we will extend the model as follows

- update nuclear shadowing for hard production of charmonium calculated from parameterization of diffractive gluon distribution function [14]
- extend nuclear absorption and its energy dependence to the whole kinematically allowed region
- include the possible recombination of $c\bar{c}$ into secondary J/ψ 's, i.e. the gain term in the differential rate equation of the model.

The latter effect is the main novel feature that will enable us to calculate the suppression pattern at RHIC, and make further predictions for the upcoming heavy-ion runs at LHC. Nuclear effects in nucleus-nucleus collisions are usually expressed through the so-called nuclear modification factor, $R_{AB}^{J/\psi}(b)$, defined as the ratio of the J/ψ yield in $A+A$ and pp scaled by the number of binary nucleon-nucleon collisions, $n(b)$. We have then

$$\begin{aligned} R_{AB}^{J/\psi}(b) &= \frac{dN_{AB}^{J/\psi}/dy}{n(b) dN_{pp}^{J/\psi}/dy} \\ &= \frac{\int d^2s \sigma_{AB}(b) n(b, s) S_{J/\psi}^{sh}(b, s) S^{abs}(b, s) S^{co}(b, s)}{\int d^2s \sigma_{AB}(b) n(b, s)}, \end{aligned} \quad (1)$$

where $\sigma_{AB}(b) = 1 - \exp[-\sigma_{pp} AB T_{AB}(b)]$, $T_{AB}(b) = \int d^2s T_A(s) T_B(b-s)$ is the nuclear overlapping function and $T_A(b)$ is obtained from Woods-Saxon nuclear densities [15]. In eq. (1),

$$n(b, s) = \sigma_{pp} AB T_A(s) T_B(b-s) / \sigma_{AB}(b), \quad (2)$$

where upon integration over d^2s we obtain the number of binary nucleon-nucleon collisions at impact parameter b , $n(b)$.

The three additional factors in the numerator of eq. (1), S^{sh} , S^{abs} and S^{co} , denote the effects of shadowing, nuclear absorption (both initial-state effects) and interaction with the co-moving matter (final-state effect), respectively. They will be defined below.

2.1 Initial-state nuclear effects

The effects related to particle production in hadronic collisions off nuclei are often called initial-state effects and have been extensively treated in the literature in the case of J/ψ production at different energies [16, 17, 18]. Since the origin and relevance of these effects is still under debate, we will present a short and updated discussion of them at both low and ultra-relativistic energies.

At low energies the primordial spectrum of particles created in scattering off a nucleus is mainly altered by **(i)** interactions with the nuclear matter they traverse on the way out to the detector and

(ii) energy-momentum conservation. The first effect is called nuclear absorption and is usually parameterized within a probabilistic Glauber model. The latter is inferred from the rapidity dependence of the spectra. For $A+A$ collisions, these effects can be combined into the following suppression factor

$$S^{abs} = \frac{[1 - \exp(-\xi(x_+)\sigma_{Q\bar{Q}}AT_A(b))] [1 - \exp(-\xi(x_-)\sigma_{Q\bar{Q}}BT_B(b-s))]}{\xi(x_+)\xi(x_-)\sigma_{Q\bar{Q}}^2ABT_A(s)T_B(b-s)}, \quad (3)$$

where $\xi(x_{\pm}) = (1 - \epsilon) + \epsilon x_{\pm}^{\gamma}$ determines both absorption and energy-momentum conservation.¹ In [16] it has been found that $\gamma = 2$, $\epsilon = 0.75$ and $\sigma_{Q\bar{Q}} = 20$ mb give a good description of data. This corresponds to $\sigma_{abs} = 5$ mb at mid-rapidity which is in agreement with other studies.

Several novel features are expected to appear at high energies due to the change in the space-time picture of particle production. First of all, the form of eq. (3) will change due to coherence effects [19]. Motivated by results from deuteron-gold collisions at $\sqrt{s} = 200$ GeV [20], it has recently been realized that this change should be accompanied by a transformation of $\xi(x_{\pm})\sigma_{Q\bar{Q}}$ into $\epsilon x_{\pm}^{\gamma}\sigma_{Q\bar{Q}}$. In this way $\sigma_{abs} = 0$ at high energies [21, 22]. Nevertheless, $S^{abs} \neq 1$ for x_{\pm} not too small, due to energy-momentum conservation. This leads to a model for the high-energy transition in which the factors in the numerator of eq. (3) are changed according to

$$\frac{1 - e^{-\xi(x_{\pm})\sigma_{Q\bar{Q}}AT_A(b)}}{\xi(x_{\pm})\sigma_{Q\bar{Q}}} \rightarrow AT_A(b) \exp[-\epsilon\sigma_{Q\bar{Q}}x_{\pm}^{\gamma}AT_A(b)/2]. \quad (4)$$

In the central rapidity region at RHIC, $x_{\pm} \sim 0.025 - 0.05$ and absorption effects can be discarded. At $|y| > 0$, $S^{abs} \neq 1$ due to energy-momentum conservation. This effect is usually neglected in the discussion of $A+A$ collisions.

Secondly, coherence effects will lead to nuclear shadowing for both soft and hard processes at RHIC, and therefore also for the production of heavy flavor. Shadowing can be calculated within the Glauber-Gribov theory [23], and we will utilize the generalized Schwimmer model of multiple scattering [24]. In this case the second suppression factor in eq. (1) is given by

$$S^{sh}(b, s, y) = \frac{1}{1 + AF(y_A)T_A(s)} \frac{1}{1 + BF(y_B)T_B(b-s)}, \quad (5)$$

where the function $F(y)$ encodes the dynamics of shadowing and will be discussed in detail below. For a general discussion of nuclear shadowing, see [25, 26].

Parameterizations of diffractive structure function from γ^*N scattering as measured at HERA have been utilized in [27] to find shadowing for sea quarks. Most recently gluon shadowing has been calculated in [28] using recent data on diffractive gluon density function [14]. Then shadowing is governed by

$$F(x, Q^2) = 4\pi \int_x^{x_P^{max}} dx_P B(x_P) \frac{F_{2D}^{(3)}(x_P, Q^2, \beta)}{F_2(x, Q^2)} F_A^2(t_{min}), \quad (6)$$

where $F(x, Q^2)$ is related to $F(y)$ in eq. (5) through kinematical relations. For gluon fusion, $x = m_T \exp(\pm y)/\sqrt{s}$. We put $x_P^{max} = 0.1$, where shadowing is expected to disappear. In eq. (6), $F_2(x, Q^2)$ is the structure function for a nucleon, $F_{2D}^{(3)}(x_P, Q^2, \beta)$ is the t-integrated diffractive structure function of the nucleon, $B(x_P)$ is the slope parameter of the distribution, and $F_A(t_{min})$ is the nuclear form factor where $t_{min} \approx -m_N^2 x_P^2$. Equation (5) determines shadowing for quarks (antiquarks) in nuclei [27]. For gluons the same expressions have been used with the substitutions: $F_{2D}^{(3)}(x_P, Q^2, \beta) \rightarrow F_{IP}^g(x_P, Q^2, \beta)$,

¹We recall that $x_{\pm} = (\sqrt{x_F^2 - 4M^2/s} \pm x_F)/2$.

$F_2(x, Q^2) \rightarrow xg(x, Q^2)$, F_P^g and g represent gluon distributions in the Pomeron, measured in diffractive deep inelastic scattering, and in the proton, respectively. We use this information to calculate shadowing for J/ψ assuming that it originates from a color octet $c\bar{c}$ pair produced in a hard gluon fusion process with $Q = m_T = 4$ GeV. The same value of Q is used for open charm production.

Since experiments at HERA mostly deal with hard diffraction and their parameterizations are quite uncertain for $Q^2 < 4$ GeV², the density of comovers, mostly low- p_\perp particles, will be calculated in the spirit of the model presented in [25, 29], where shadowing corrections are given without free parameters in terms of the triple-Pomeron coupling determined from diffraction data. Then, in eq. (5)

$$F(y_A) = C_{sh} \left[\exp(\Delta Y_{max}^A) - \exp(\Delta Y_{min}^A) \right], \quad (7)$$

where $Y_{min}^A = \ln(R_A m_N / \sqrt{3})$, $\Delta = 0.13$ and $C_{sh} = 0.31$ fm². The value of Y_{max} depends on the rapidity of the produced particle h , $Y_{max}^A = \ln(s/m_T^2)/2 \pm y$ with the $+(-)$ sign if h is produced in the hemisphere of nucleus $B(A)$. m_T is the transverse mass of the produced particle. We use $m_T = 0.4$ GeV at RHIC and 0.5 GeV at LHC. This model has been used to correctly predict the centrality dependence of soft particle production at RHIC [29].

The energy dependence of these different effects can be summarized as follows. Particle production at SPS is dominated by low-energy effects, i.e. nuclear absorption given by eq. (3) and small nuclear shadowing, while RHIC already belongs to the high-energy regime. Nuclear shadowing is non-negligible at mid-rapidity, and the combined effect of shadowing and energy-momentum conservation, in the spirit of eq. (4), should be accounted for at forward rapidities. At LHC, shadowing will be very strong even at $y = 0$ while energy-momentum conservation is a small effect and can be neglected in most of the kinematics. We will now proceed with the discussion of final state effects.

2.2 Dissociation by comovers interaction and recombination

The CIM was developed to explain both the suppression of charmonium yields [3, 10, 30, 31, 32, 33, 34] and the strangeness enhancement [35, 36] in nucleus-nucleus collisions at the SPS. Neglecting possible recombination effects, the rate equation governing the density of charmonium in the final state, $N_{J/\psi}$, can be written in a simple form assuming a pure longitudinal expansion of the system and boost invariance. For an $A+A$ collision the density of J/ψ at a given transverse coordinate, s , impact parameter b , and rapidity is given by

$$\tau \frac{dN_{J/\psi}}{d\tau}(b, s, y) = -\sigma_{co} N^{co}(b, s, y) N_{J/\psi}(b, s, y), \quad (8)$$

where σ_{co} is the cross section of charmonium dissociation due to interactions with the co-moving medium, with density N^{co} . It is found from fits to low-energy experimental data to be $\sigma_{co} = 0.65$ mb [3]. To incorporate the effects of recombination, we have to include an additional gain term proportional to the (squared) density of open charm produced in the collision. Then eq. (8) is generalized to

$$\tau \frac{dN_{J/\psi}}{d\tau}(b, s, y) = -\sigma_{co} \left[N^{co}(b, s, y) N_{J/\psi}(b, s, y) - N_c(b, s, y) N_{\bar{c}}(b, s, y) \right], \quad (9)$$

where we have assumed that the effective recombination cross section is equal to the dissociation cross section.² This extension of the model therefore does not involve additional parameters.

Equation (9) cannot be solved analytically. We approximate its solution as

$$S^{co}(b, s, y) = \exp \left\{ -\sigma_{co} \left[N^{co}(b, s, y) - \frac{N_c(b, s, y) N_{\bar{c}}(b, s, y)}{N_{J/\psi}(b, s, y)} \right] \ln \left[\frac{N^{co}(b, s, y)}{N_{pp}(0)} \right] \right\}, \quad (10)$$

²These two cross-sections have to be similar but not necessarily equal. We have taken the simplest possibility.

resembling the exact solution of eq. (8), since the first term in the exponent of eq. (10) is exactly the survival probability of a J/ψ interacting with comovers [10]. The density of open and hidden charm in $A+A$ collisions, $N_c, N_{\bar{c}}$ and $N_{J/\psi}$, respectively, can be computed from their densities in pp collisions as $N_c^{AA}(b, s) = n(b, s)S_{HQ}^{sh}(b, s)N_c^{pp}$, with similar expression for $N_{\bar{c}}^{AA}$ and $N_{J/\psi}^{AA}$. Here $n(b, s)$ is given by eq. (2) and S_{HQ}^{sh} is the shadowing factor for heavy quark production, given by eq. (6). Then eq. (10) becomes

$$S^{co}(b, s, y) = \exp \left\{ -\sigma_{co} \left[N^{co}(b, s, y) - C(y)n(b, s)S_{HQ}^{sh}(b, s) \right] \ln \left[\frac{N^{co}(b, s, y)}{N_{pp}(0)} \right] \right\} \quad (11)$$

where

$$C(y) = \frac{\left(\frac{dN_{pp}^{c\bar{c}}}{dy} \right)^2}{dN_{pp}^{J/\psi}/dy} = \frac{\left(\frac{d\sigma_{pp}^{c\bar{c}}}{dy} \right)^2}{\sigma_{pp} d\sigma_{pp}^{J/\psi}/dy} . \quad (12)$$

The quantities in the rightmost term in eq. (12) are all related to pp collisions at the corresponding energy and can be taken from experiment or a model (for extrapolation of the experimental results). The $c\bar{c}$ pairs are mostly in charmed mesons, such as D and D^* . With σ_{co} fixed from experiments at low energy, where recombination effects are negligible, the model, formulated above, should be self-consistent at high energies³. We expect the effect of recombination to be stronger at mid- than at forward rapidities. At $y \neq 0$ the recombination term is smaller (relative to the first one) since the rapidity distribution of D, D^* is narrower than the one of comovers. This will produce a decrease of $R_{AA}^{J/\psi}$ with increasing y which may over-compensate the increase due to a smaller density of comovers at $y \neq 0$.

The density of comovers is calculated using the dual parton model [37] together with the proper shadowing correction. Then

$$N^{co}(b, s, y) = N_{NS}^{co}(b, s, y) S_{ch}^{sh}(b, s, y) , \quad (13)$$

where S_{ch}^{sh} denotes the shadowing for light particles and is given by eqs. (5) and (7). The non-shadowed (NS) multiplicity of comovers is then

$$N_{NS}^{co}(b, s, y) = \frac{3}{2} \frac{dN_{NS}^{ch}(b, s, y)}{dy} = \frac{3}{2} \{ C_1(b, y)n_A(b, s) + C_2(b, y)n(b, s) \} , \quad (14)$$

where

$$n_A(b, s) = \frac{AT_A(s)}{\sigma_{AB}(b)} [1 - \exp(-\sigma_{pp}BT_B(b-s))] , \quad (15)$$

and $n(b, s)$ is given by eq. (2). The numerical values of the coefficients C_1 and C_2 can be found in [10]. C_1 drops with energy while C_2 increases, and at LHC $C_1 \approx 0$ while $C_2 \approx 6$ at mid-rapidity. Also in eq. (10) $N_{pp}(0) = \frac{3}{2} \left(\frac{dN^{ch}}{dy} \right)_{y=0}^{pp} / \pi R_p^2$, which we estimate⁴ to be 2.24 fm^{-2} at $\sqrt{s} = 200 \text{ GeV}$ and 4.34 fm^{-2} at $\sqrt{s} = 5.5 \text{ TeV}$. Finally, σ_{pp} , taken as its non-diffractive value, is 34 mb and 59 mb at RHIC and LHC, respectively.

³Note, however, that σ_{co} could change when the energy increases. We do not expect this effect to be important and, since we are unable to evaluate the magnitude of this eventual change, we shall use the same value $\sigma_{co} = 0.65 \text{ mb}$ at all energies.

⁴ pp values at LHC of dN/dy and σ are based on DPMJET-III calculations. We thank J. Ranft for providing these results.

3 Charmonium production at RHIC

At RHIC, the dissociation term alone gives a too strong suppression compared to experimental data [10]. We therefore proceed to estimate the effect of recombination. The density of open charm at mid-rapidity in pp collisions at $\sqrt{s} = 200$ GeV has been reported in [38] and the most recent measurement of the J/ψ density in [39]. We present results of experimental measurements in Table 1. The semi-leptonic branching ratio for the J/ψ is $B_{ll} = 0.059$. Then, from eq. (12) it follows that $C = 0.59$ at mid-rapidities. One has to keep in mind, however, that the measured yield of open charm at RHIC is almost twice as large as predictions from pQCD [40]. In the left picture of Fig. 1 we present the results of our model compared to experimental data at mid-rapidity. The different contributions to J/ψ suppression are shown (see figure caption). Note that at mid-rapidities the initial-state effect is just the shadowing. As discussed above nuclear absorption due to energy-momentum conservation is present at forward rapidities but is negligibly small at mid-rapidities.

Measurements of open charm at forward rapidities [41] have too large systematic errors at the moment. Therefore, to estimate the density of charm at forward rapidity we use results of PYTHIA [42] with parameters and settings as described in [41]. The resulting rapidity distributions can be described by slightly broadened Gaussian functions. Note, that with this PYTHIA value, given in Table 1, the ratio of open charm production at mid- and forward rapidities is very similar to the one measured for J/ψ production. With these values of J/ψ and open charm rapidity distributions we get $C = 0.32$ at forward rapidities. Using this value of C and a ratio of 1.2 [43] of the comover densities $N^{c\bar{c}}$ between $y = 0$ and y forward we obtain the curve in the r.h.s. of Fig. 1. We note that no free parameters were tuned to obtain these results. Note that, contrary to the results in [10] with no recombination, the J/ψ suppression at forward rapidity is somewhat larger than the one at mid-rapidities, in agreement with experimental data. This is due both to the recombination term and to the initial-state effects. The latter are stronger for forward rapidities. They include the effects of energy-momentum conservation, which were not considered in [10].

For consistency, we have also made calculations for the J/ψ suppression in $Cu+Cu$ collisions at RHIC which was reported in [13], using the same parameters as above for $Au+Au$ collisions. The results are shown in Fig. 2, and are in good agreement with the experimental data, except for peripheral collisions where the error bars are quite large.

Concluding, our procedure gives a reasonable description of data both at mid- and forward rapidity for different collision systems at RHIC, in contrast with the recent claim [44] that the CIM fails to reproduce forward rapidity data. We have shown that the situation is much improved by inclusion of a recombination term.

4 Predictions for LHC

Based on our previous discussion, it is obvious that recombination effects will be of crucial importance in $Pb+Pb$ collisions at LHC ($\sqrt{s} = 5.5$ TeV). Assuming that the energy dependence of open charm and J/ψ in pp collisions is the same (between RHIC and LHC energies), the energy dependence of the parameter C will be that of $\sigma_{pp}^{c\bar{c}}/\sigma_{pp}$. The total and differential cross section for charm can be calculated using perturbative techniques [40, 45]. The calculations for low energies are in agreement with data, yet predictions for RHIC and Tevatron energies are lower than the data. Therefore, the extrapolation to LHC is quite uncertain. If we parameterize the energy dependence of open charm production as $\sigma^{c\bar{c}} \propto s^\alpha$, with $\alpha = 0.3$ and use the values of non-diffractive σ_{pp} given at the end of Section 2 we obtain $C = 2.5$ at LHC – a value about four times larger than the corresponding one at RHIC. In view of that we consider that realistic values of C at LHC are of the range 2 to 3. In Fig. 3 we have calculated the J/ψ suppression at LHC for several values of C , including the case of absence

of recombination effects ($C = 0$). Although the density of charm grows substantially from RHIC to LHC, the combined effect of initial-state shadowing and comovers dissociation appears to overcome the effect of parton recombination. This is in sharp contrast with the findings of [6], where a strong enhancement of the J/ψ yield with increasing centrality was predicted.

It is clear that a better theoretical control is needed on the various factors that are included in C . As discussed in Section 2 the comovers cross section σ_{co} can vary a little with energy. But the most important theoretical input at the moment is the energy dependence of the total charm cross section in pp collisions.

5 Conclusion

In this work we have incorporated the effects of recombination of $c\bar{c}$ pairs into J/ψ in the comovers interaction model. These effects are negligible at low energies (SPS) due to the low density of open charm. This model does not assume thermal equilibrium of the matter produced in the collision and includes a comprehensive treatment of initial-state effects, such as shadowing, nuclear absorption and energy-momentum conservation.

We estimate the magnitude of the recombination term from J/ψ and open charm yields in pp collisions at RHIC. Without any adjustable parameters, the centrality and rapidity dependence of experimental data is reproduced both for $Au+Au$ and $Cu+Cu$ collisions.

Finally, we make predictions for future measurements of J/ψ in $Pb+Pb$ collisions at LHC. In our approach, the magnitude of the recombination effect is controlled by the total charm cross section in pp collisions, and therefore our predictions are strongly dependent on input from theoretical models at these energies. For a reasonable choice of parameters, we predict that the suppression observed at RHIC and lower energies will still dominate over the recombination effects. This is due to the large density of comovers and to the strong initial-state suppression at these ultra-relativistic energies.

Acknowledgments

This work was supported by the Norwegian Research Council (NFR) under contract No. 166727/V30, RFBF-06-02-17912, RFBF-06-02-72041-MNTI, INTAS 05-103-7515, grant of leading scientific schools 845.2006.2 and Federal Agency on Atomic Energy of Russia.

References

- [1] T. Matsui, H. Satz, Phys. Lett. B **178**, 416 (1986)
- [2] B. Alessandro, et al., Eur. Phys. J. C **39**, 335 (2005)
- [3] N. Armesto, A. Capella, E.G. Ferreira, Phys. Rev. C **59**, 395 (1999)
- [4] R. Thews, M. Schroedter, J. Rafelski, Phys. Rev. C **63**, 054905 (2001)
- [5] L. Grandchamp, R. Rapp, Nucl. Phys. A **709**, 415 (2002)
- [6] P. Braun-Munzinger, J. Stachel, Phys. Lett. B **490**, 196 (2000)
- [7] A. Andronic, P. Braun-Munzinger, K. Redlich, J. Stachel, Phys. Lett. B **571**, 36 (2003)
- [8] A.P. Kostyuk, M.I. Gorenstein, H. Stöcker, W. Greiner, Phys. Rev. C **68**, 041902 (2003)

- [9] L. Yan, P. Zhuang, N. Xu, Phys. Rev. Lett. **97**, 232301 (2006)
- [10] A. Capella, E.G. Ferreira, Eur. Phys. J. C **42**, 419 (2005)
- [11] A. Adare, et al., Phys. Rev. Lett. **98**, 232301 (2007)
- [12] M.J. Leitch, J. Phys. G **34**, S453 (2007), nucl-ex/0701021
- [13] V. Cianciolo, AIP Conf. Proc. **842**, 41 (2006), nucl-ex/0601012
- [14] A. Aktas, et al., Eur. Phys. J. C **48**, 715 (2006); *ibid.* **48**, 749 (2006)
- [15] C.W. De Jager, H. De Vries and C. De Vries, Atom. Data Nucl. Data Tabl. **14**, 479 (1974)
- [16] K.G. Boreskov, A.B. Kaidalov, in *Proceedings of the XXVth Rencontre de Moriond, Savoie, 1991*, edited by J. Tran Thanh Van, (Editions Frontieres, 1991)
K.G. Boreskov, A. Capella, A.B. Kaidalov, J. Tran Thanh Van, Phys. Rev. D **47**, 919 (1993)
- [17] D. Kharzeev, C. Lourenço, M. Nardi, H. Satz, Z. Phys. C **74**, 307 (1997)
- [18] R. Vogt, Phys. Rev. C **71**, 054902 (2005)
- [19] M.A. Braun, C. Pajares, C.A. Salgado, N. Armesto, A. Capella, Nucl. Phys. B **509**, 357 (1998)
- [20] S.S. Adler, et al., Phys. Rev. Lett. **96**, 012304 (2006)
- [21] A. Capella, E.G. Ferreira, hep-ph/0610313
- [22] I.C. Arsene, L. Bravina, A.B. Kaidalov, K. Tywoniuk, E. Zabrodin, Phys. Lett. B (in press), arXiv:0711.4672 [hep-ph]
K. Tywoniuk, et al., J. Phys. G (in press), arXiv:0712.2382 [hep-ph]
- [23] V.N. Gribov, Sov. Phys. JETP **29**, 483 (1969); *ibid.* **30**, 709 (1970); *ibid.* **26**, 414 (1968)
- [24] A. Schwimmer, Nucl. Phys. B **94**, 445 (1975)
- [25] A. Capella, A. Kaidalov, J. Tran Thanh Van, Heavy Ion Phys. **9**, 169 (1999), hep-ph/9903244
- [26] N. Armesto, J. Phys. G **32**, R367 (2006)
- [27] N. Armesto, A. Capella, A.B. Kaidalov, J. Lopez-Albacete, C.A. Salgado, Eur. Phys. J. C **29**, 531 (2003)
- [28] K. Tywoniuk, I. Arsene, L. Bravina, A. Kaidalov, E. Zabrodin, Phys. Lett. B **657**, 170 (2007); Eur. Phys. J. C **49**, 193 (2007)
- [29] A. Capella, D. Sousa, Phys. Lett. B **511**, 185 (2001)
- [30] S. Brodsky, A.H. Mueller, Phys. Lett. B **206**, 685 (1988)
- [31] B. Koch, U. Heinz, J. Pitsut, Phys. Lett. **243**, 149 (1990)
- [32] A. Capella, A. Kaidalov, A. Kouider Akil, C. Gerschel, Phys. Lett. B **393**, 431 (1997)
- [33] N. Armesto, A. Capella, Phys. Lett. B **430**, 23 (1998)
- [34] A. Capella, E.G. Ferreira, A.B. Kaidalov, Phys. Rev. Lett. **85**, 2080 (2000)

- [35] A. Capella, Phys. Lett. B **364**, 175 (1995)
- [36] A. Capella, A. Kaidalov, A. Kouider Akil, C. Merino, J. Tran Thanh Van, Z. Phys. C **70**, 507 (1996)
A. Capella, C.A. Salgado, D. Sousa, Eur. Phys. J. C **30**, 111 (2003)
- [37] A. Capella, U. Sukhatme, C.I. Tan, J. Tran Thanh Van, Phys. Rept. **236**, 225 (1994)
- [38] A. Adare, et al., Phys. Rev. Lett. **97**, 252002 (2006)
- [39] A. Adare, et al., Phys. Rev. Lett. **98**, 232002 (2007)
- [40] M. Cacciari, P. Nason, R. Vogt, Phys. Rev. Lett. **95**, 122001 (2005)
- [41] S.S. Adler, et al., Phys. Rev. D **76**, 092002 (2007)
- [42] T. Sjostrand, P. Eden, C. Friberg, L. Lonnblad, G. Miu, S. Mrenna, E. Norrbin, Comput. Phys. Commun. **135**, 238 (2001)
- [43] R. Debbe, AIP Conf. Proc. **870**, 707 (2006), `nuc1-ex/0608048`
- [44] O. Linnyk, E.L. Bratkovskaya, W. Cassing, H. Stöcker, Phys. Rev. C **76**, 041901 (2007)
- [45] R. Vogt, `arXiv:0709.2531 [hep-ph]`

List of Figures

1	Results for J/ψ suppression in $Au+Au$ at RHIC ($\sqrt{s} = 200$ GeV) at mid- (left figure), and at forward rapidities (right figure). Data are from [11]. The solid curves are the final results. The dashed-dotted ones are the results without recombination ($C = 0$). The dashed line is the total initial-state effect. The dotted line in the right figure is the result of shadowing. In the left figure the last two lines coincide (see main text). . . .	12
2	Results for J/ψ suppression in $Cu+Cu$ at RHIC ($\sqrt{s} = 200$ GeV), at mid- (left) and at forward rapidities (right). For details, see caption of Fig. 1. Data are from [13]. . . .	13
3	Results for J/ψ suppression in $Pb+Pb$ at LHC ($\sqrt{s} = 5.5$ TeV) at mid-rapidities for different values of the parameter C . The upper line is the suppression due to initial-state effects (shadowing).	14

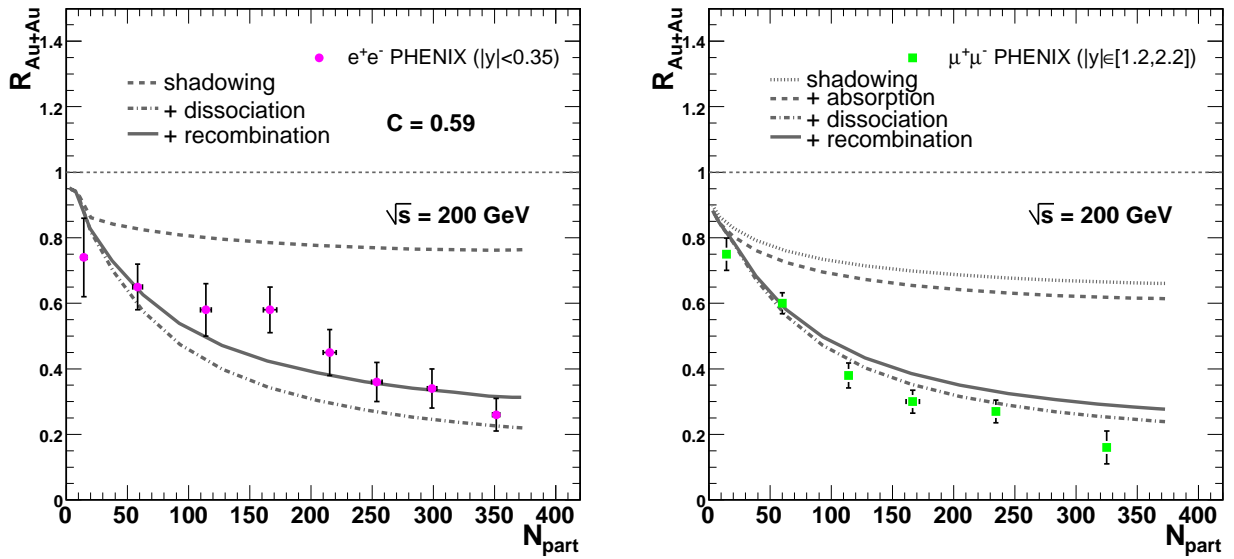


Figure 1: Results for J/ψ suppression in $Au+Au$ at RHIC ($\sqrt{s} = 200$ GeV) at mid- (left figure), and at forward rapidities (right figure). Data are from [11]. The solid curves are the final results. The dashed-dotted ones are the results without recombination ($C = 0$). The dashed line is the total initial-state effect. The dotted line in the right figure is the result of shadowing. In the left figure the last two lines coincide (see main text).

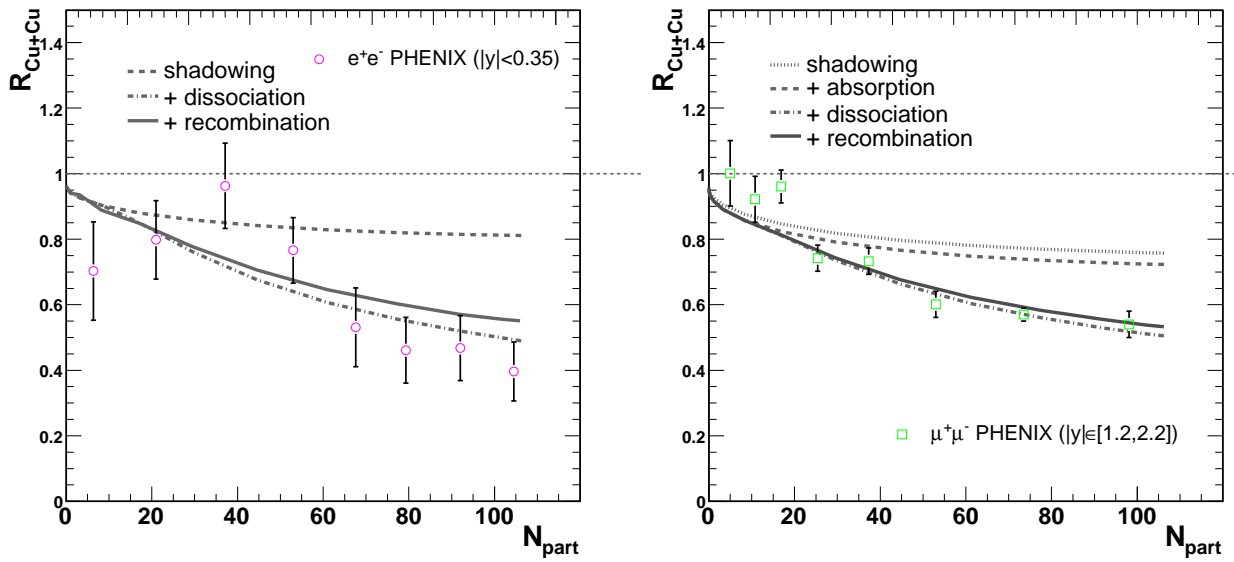


Figure 2: Results for J/ψ suppression in $Cu+Cu$ at RHIC ($\sqrt{s} = 200$ GeV), at mid- (left) and at forward rapidities (right). For details, see caption of Fig. 1. Data are from [13].

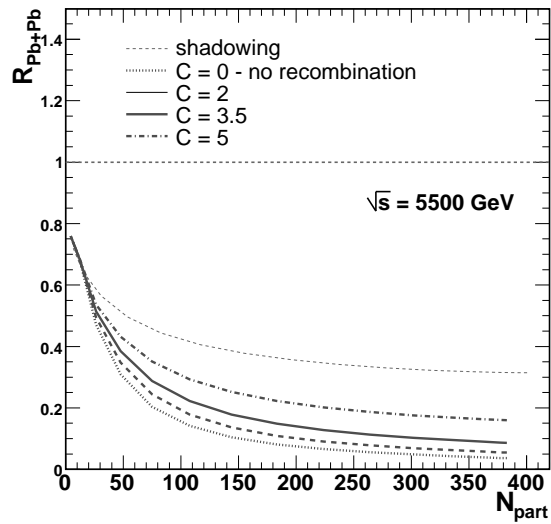


Figure 3: Results for J/ψ suppression in $Pb+Pb$ at LHC ($\sqrt{s} = 5.5$ TeV) at mid-rapidities for different values of the parameter C . The upper line is the suppression due to initial-state effects (shadowing).

List of Tables

- 1 Open charm and J/ψ production cross sections in pp collisions at $\sqrt{s} = 200$ GeV. Data are taken from [38, 39, 41]. 16

Table 1: Open charm and J/ψ production cross sections in pp collisions at $\sqrt{s} = 200$ GeV. Data are taken from [38, 39, 41].

	$(d\sigma_{pp}^{c\bar{c}}/dy)_{EXP}$	$(d\sigma_{pp}^{c\bar{c}}/dy)_{PYTHIA}$	$(B_{ll} d\sigma_{pp}^{J/\psi}/dy)_{EXP}$
mid-rap	$123 \pm 12 \pm 45 \mu\text{b}$		$44.3 \pm 1.4 \pm 5.1 \text{ nb}$
forward		$70.9 \pm 14 \mu\text{b}$	$27.61 \pm 0.37 \pm 0.83 \text{ nb}$